We are IntechOpen, the world's leading publisher of Open Access books Built by scientists, for scientists

4,800
Open access books available

122,000
International authors and editors

135M
Downloads

Our authors are among the

154
Countries delivered to

TOP 1%
most cited scientists

12.2%
Contributors from top 500 universities

WEB OF SCIENCE™

Selection of our books indexed in the Book Citation Index in Web of Science™ Core Collection (BKCI)

Interested in publishing with us?
Contact book.department@intechopen.com

Numbers displayed above are based on latest data collected.
For more information visit www.intechopen.com

25

Type Design of Decoupled Parallel Manipulators with Lower Mobility

Weimin Li
School of Mechanical Engineering, Hebei University of Technology
P. R. China

1. Introduction

A typical parallel mechanism consists of a moving platform, a fixed base, and several kinematical chains (also called the legs or limbs) which connect the moving platform to its base. Only some kinematical pairs are actuated, whose number usually equals to the number of degrees of freedom (dofs) that the platform possesses with respect to the base. Frequently, the number of legs equals to that of dofs. This makes it possible to actuate only one pair per leg, allowing all motors to be mounted close to the base. Such mechanisms show desirable characteristics, such as large payload and weight ratio, large stiffness, low inertia, and high dynamic performance. However, compared with serial manipulators, the disadvantages include lower dexterity, smaller workspace, singularity, and more noticeable, coupled geometry, by which it is very difficult to determine the initial value of actuators while the end effector stands at its original position.

In an engineering point of view, it is always important to develop a simple and efficient original position calibration method to determine initial values of all actuators. This calibration method usually becomes one of the key techniques that a type of mechanism can be simply and successfully used to the precision applications. Accordingly, few have been reported that the parallel manipulators being applied to high precision situations except micro-movement ones.

The study of movement decoupling for parallel manipulators shows an opportunity to simply the original position calibration and to improve the precision of parallel manipulators in a handy way. One of the most important things in the study of movement decoupling of parallel manipulators is how to design a new type with decoupled geometry.

Decoupled parallel manipulators with lower mobility (LM-DPMs) are parallel mechanisms with less than six dofs and with decoupled geometry. This type of manipulators has attracted more and more attention of academic researchers in recent years. Till now, it is difficult to design a decoupled parallel manipulator which has translational and rotational movement simultaneously (Zhang et al., 2006a, 2006b, 2006c). Nevertheless, under some rules, it is relatively easy to design a decoupled parallel manipulator which can produce pure translational (Baron & Bernier, 2001; Carricato, & Parenti-Castelli, 2001a; Gao et al., 2005; Hervé, & Sparacino, 1992; Kim & Tsai, 2003; Kong & Gosselin, 2002; Li et al., 2005a, 2005b, 2006a; Tsai, 1996; Tsai et al., 1996; Zhao & Huang, 2000) or rotational (Carricato & Parenti-Castelli, 2001b, 2004; Gogu, 2005; Li et al., 2006b, 2007a, 2007b) movements.

Source: Parallel Manipulators, New Developments, Book edited by: Jee-Hwan Ryu, ISBN 978-3-902613-20-2, pp. 498, April 2008, I-Tech Education and Publishing, Vienna, Austria

This chapter attempts to provide a unified frame for the type design of decoupled parallel manipulators with pure translational or rotational movements.
The chapter starts with the introduction of the LM-DPMs, and then, introduce a general idea for type design. Finally, divide the specific subjects into two independent aspects, pure translational and rotational. Each of them is discussed separately. Special attention is paid to the kinds of joins or pairs, the limb topology, the type design, and etc.

2. The general idea for decoupled parallel manipulators with lower mobility

The general idea for the type design of decoupled parallel manipulators with lower mobility can be expressed as the following theory.
Theory: A movement is independent with others if one of the following conditions is satisfied:
(1) To the pure translational mechanisms, the translational actuator is orthogonal with the plane composed of other translational actuators.
(2) To the pure rotational mechanisms (spherical mechanisms), the translational actuator is parallel with the axis of rotational actuator.

Depend on part (1) of the theory, we can design some kinds of 3-dofs pure translational decoupled parallel manipulators. Also we can get some kinds of 2-dofs spherical mechanism based on part (2) of the theory.
For the convenience, first, let us define some letters to denote the joints (or pairs). They are the revolute joint (R), the spherical joint (S), the prismatic pair (P), and the planar pair or flat pair (F). They possess one revolute dof, three revolute dofs, one translational dof and three dofs (two translational and one revolute) respectively. Then the theory can be expressed by figure 1 and figure 2 separately.
Figure 1 illustrates the limb topology. The actuator should be installed with the prismatic pair. The flat pair can be composed in deferent way. Using this kind of limb, we can design some kinds of 3-dofs pure translational decoupled parallel manipulators.

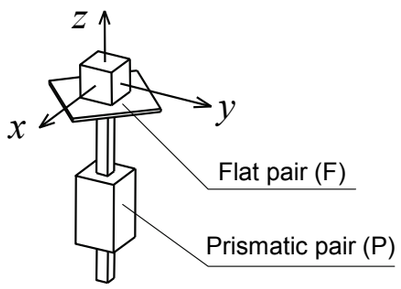

Fig. 1. The idea for limb which can be used to compose decoupled translational mechanisms

Figure 2(a) illustrates the general one geometry of a decoupled 2-dofs spherical mechanism. The moving platform is anchored to the base by two legs. A leg consists of two revolute joints, R_1 and R_2, whose axes, z_1 and z_2, intersect at point o and connect to each other perpendicularly to form a universal joint; so the value of α is $\pi/2$. The other leg consists of a revolute joint, R_3, a flat pair, F, and a prismatic pair P, in which the moving direction of P is perpendicular to the working plane of F and the axis of R_3. The revolute joints R_2 and R_3 are mounted on the moving platform in parallel. The prismatic pair P and the revolute joint R_1 are assembled to the base, in which the moving direction of P is parallel to the axis of R_1.

Suppose that the input parameters, q_1 and q_2, represent the positions of the revolute joint R_1 and the prismatic pair P, which are driven by a rotary actuator and a linear actuator separately. The pose of the moving platform is defined by the Euler angles θ_1 and θ_2 of the platform. When the value of q_1 changes and q_2 holds the line, only θ_1 alters. On the other hand, when the value of q_2 changes, only θ_2 changes. So, θ_1 and θ_2 are independently determined by q_1 and q_2 respectively, i.e., one output parameter only relates to one input parameter. In other words, the platform rotations around two axes are decoupled.
Figure 2(b) is an improved idea of figure 2(a). Using this idea, we can get a decoupled 2-dofs spherical mechanism with a hemi-sphere work space.

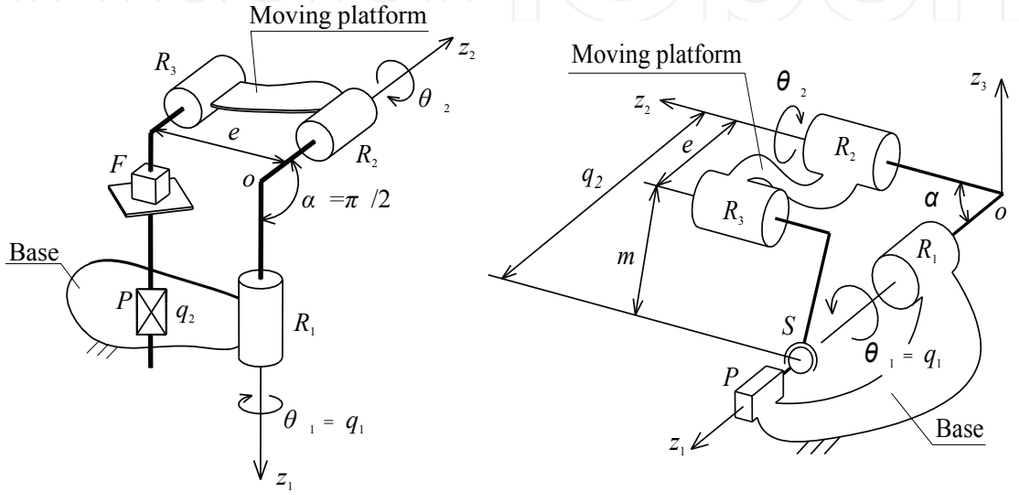

Fig. 2. The idea for decoupled 2-dof spherical mechanisms

3. Design of 3-dofs translational manipulators with decoupled geometry

3.1 Type design

The Type design of 3-dofs translational manipulators is based on the analysis of limb topology shown in figure 1.

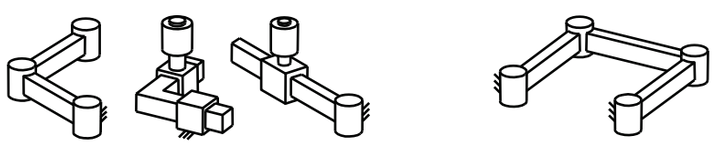

(a) flat pair (3R, PPR, RPR) (b) prismatic pair (4R)

Fig. 3. The substitutes for the flat pair and the prismatic pair

Firstly, we construct deferent structures to replace the flat pair and the prismatic pair. Some substitutes for the flat pair and the prismatic pair are shown in figure 3. Then, using the pairs to form variational kinds of limbs. Figure 4 shows three examples. Finally, we can constitute the 3-dofs translational manipulators by installing the specified limbs in orthogonal as shown in figure 5, 6 and 7.

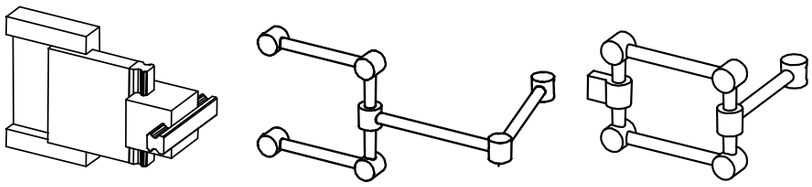

(a) PPP (b) 7R (c) Modified 7R

Fig. 4. The examples of limbs

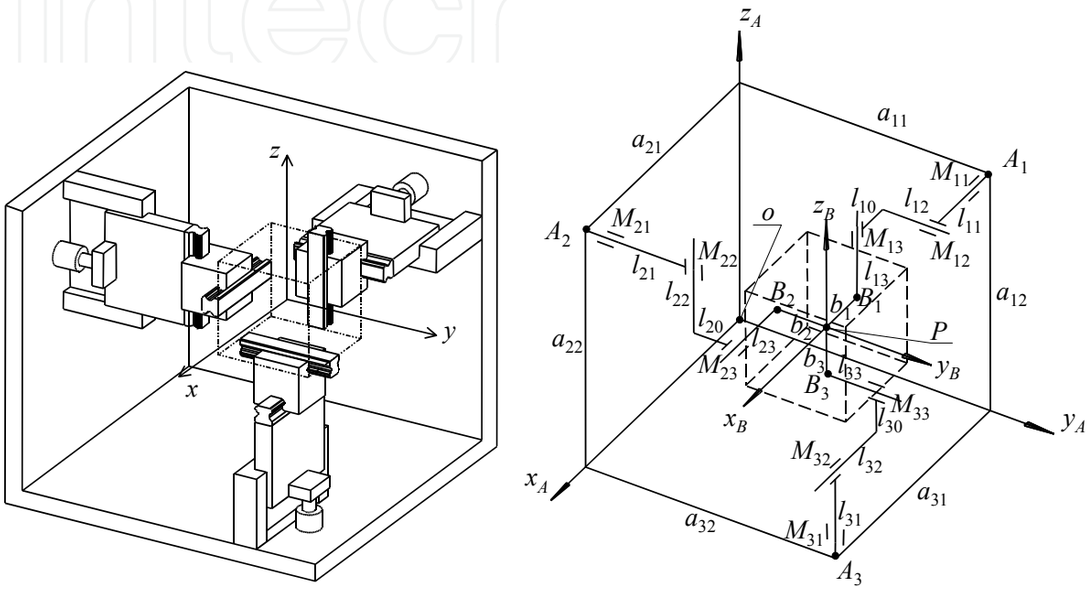

(a) Structure (b) Geometry

Fig. 5. 3-PPP manipulator

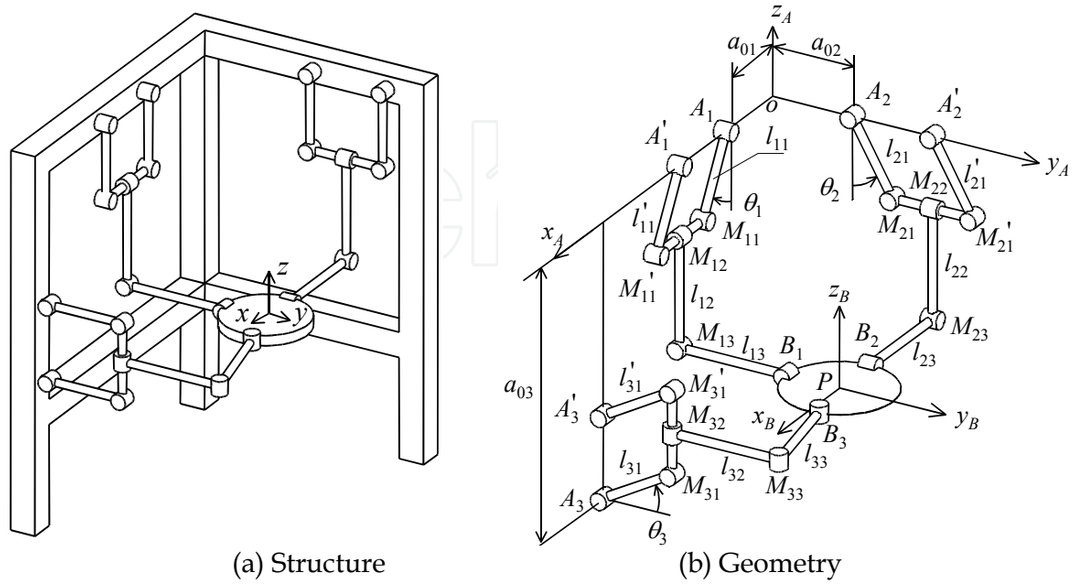

(a) Structure (b) Geometry

Fig. 6. 3-7R manipulator

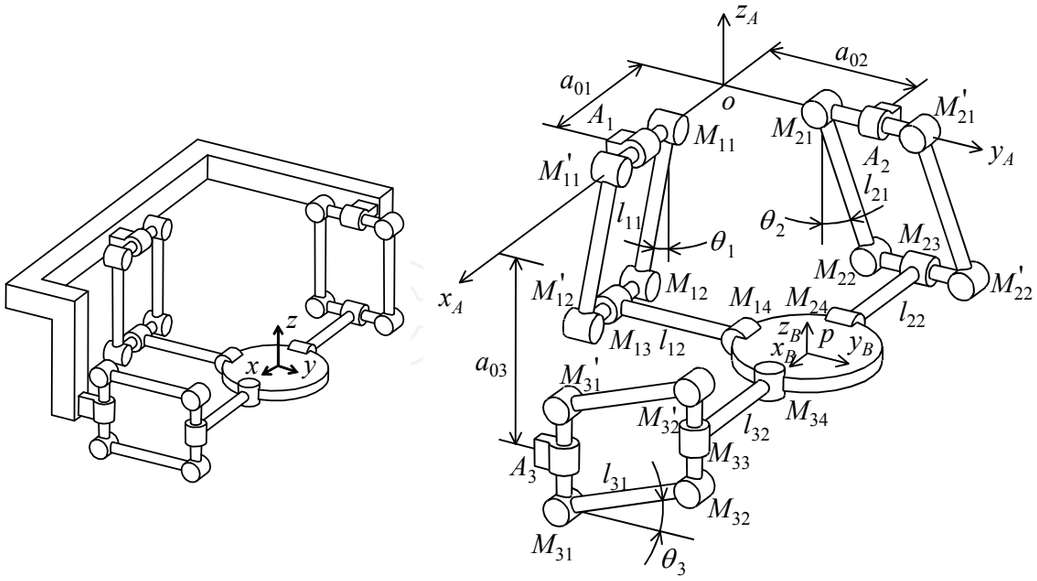

(a) Structure (b) Geometry

Fig. 7. Modified 3-7R manipulator

3.2 Kinematics

The forward and inverse kinematic analyses for the 3-PPP manipulator shown in figure 5 are trivial since there exists a one-to-one correspondence between the moving platform position and the input pair displacements. So the velocity jacobia matrix is a 3×3 identity matrix.

The kinematics of 3-7R manipulator can be analysed as follows. Referring to figure 6(b), each limb constrains point P to lie on a plane which passes through points M_{j2}, M_{j3}, and B_j, and is perpendicular to the axis of x, y, and z, respectively. The position of j^{th} plane is determined only by θ_j whenever the length l_{j1} is given. Consequently, the position of P is determined by the intersection of three planes, i.e., the intersection of θ_j for j=1,2,3. If the distance from M_{j1} to M_{j2} is m_{0j}, then a simple kinematic relation can be written as

$$\begin{bmatrix} p_x \\ p_y \\ p_z \end{bmatrix} = \begin{bmatrix} a_{01} + m_{01} + l_{11}\sin\theta_1 \\ a_{02} + m_{02} + l_{21}\sin\theta_2 \\ -a_{03} + m_{03} + l_{31}\sin\theta_3 \end{bmatrix} \tag{1}$$

where $\mathbf{p}=[p_x\ p_y\ p_z]^T$ denotes the position vector of the end-effector. Taking the time derivative of equation (1) yields

$$\begin{bmatrix} \dot{\theta}_1 \\ \dot{\theta}_2 \\ \dot{\theta}_3 \end{bmatrix} = J^{-1} \begin{bmatrix} \dot{p}_x \\ \dot{p}_y \\ \dot{p}_z \end{bmatrix} \tag{2}$$

where J is a diagonal matrix that holds

$$J = \begin{bmatrix} l_{11}\cos\theta_1 & & \\ & l_{21}\cos\theta_2 & \\ & & l_{31}\cos\theta_3 \end{bmatrix} \tag{3}$$

The kinematics of the modified 3-7R manipulator are the same.

3.3 Original position calibration

The calibration of 3-PPP manipulator is the same as a pure translational 3-dofs serial manipulator. So we just consider the manipulator of 3-7R and modified 3-7R, they can be expressed in the same way as shown in figure 8(a).

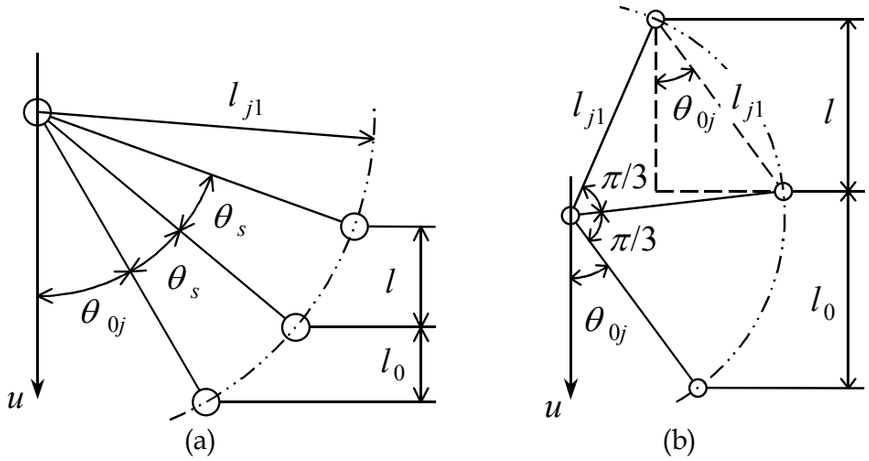

Fig. 8. Original position calibration

For convenience, we suppose,
(1) The input θ_j (j=1,2,3) is within [$-\theta_{jm}$, θ_{jm}], where θ_{jm} >0, and $\theta_j = \theta_{jm}$ denotes the initial position of the j^{th} limb;
(2) In the initial position (see figure 8), the angle between the link l_{j1} (j=1,2,3) and the axis u(u=x,y,z) is θ_{0j} (j=1,2,3).
Then the initial value θ_{jm} of θ_j can be determined as

$$\theta_{jm} = \frac{\pi}{2} - \theta_{0j} \tag{4}$$

So we can determine θ_{0j} first, then θ_{jm}, the steps of the calibration can be as follows. From the initial position θ_{0j} of the arm in figure 8, rotate the driving arm twice in a specified angle θ_s, which satisfies

$$2\theta_s + \theta_{0j} \le \pi \tag{5}$$

During the process, record the two moving distances l_0 and l of the platform in the direction of axis u(u=x,y,z), they satisfy

$$\begin{cases} l_{j1}\cos\theta_{0j} - l_{j1}\cos(\theta_{0j} + \theta_s) = l_0 \\ l_{j1}\cos\theta_{0j} - l_{j1}\cos(\theta_{0j} + 2\theta_s) = l_0 + l \end{cases} \tag{6}$$

expand $\cos(\theta_{0j}+\theta_s)$ and $\cos(\theta_{0j}+2\theta_s)$ in equation (6), and eliminate $\sin\theta_{0j}$, we get

$$\cos\theta_{0j}=\frac{l_0+l-2l_0\cos\theta_s}{2l_{j1}(1-\cos\theta_s)} \tag{7}$$

If $\theta_0 \le \pi/3$ and let $\theta=\pi/3$, then equation (7) yields

$$\cos\theta_{0j}=\frac{l}{l_{j1}} \tag{8}$$

The geometric signification of the equation (8) is shown in figure 8(b), which is very sententious and convenient to industrial applications. θ_{jm} can be get from equation (4).

3.4 Singularity

The 3-PPP manipulator has no singularity, so we just discuss the manipulator of 3-7R and modified 3-7R, they can be expressed in the same.

From equation (2) we can find out that the rotational actuator speed is nonlinear to the velocity of the end-effector. Moreover, if $\theta_j=\pm 90°$, then $\det|J|=0$, for any expected velocity of the end-effector, the rotational speed of the actuator will be infinite. When θ_j is not equal but close to $\pm 90°$, then $\det|J|\to 0$, the required rotational speed of the actuator may be still too high to reach. So the value of the θ_j must be designed in an appropriate range whenever the speed limit of the end-effector is given.

Suppose the desired velocity of the end-effector is v_e, and the permissible rotational speed of the actuator is n_e, then the absolute maximum value of the θ_j for $j=1,2,3$ can be obtained from equation (2), that is

$$\cos|\theta_j|=\frac{v_e}{l_{j1}n_e} \tag{9}$$

Let

$$\theta_{jm}=\arccos\frac{v_e}{l_{j1}n_e} \tag{10}$$

Then θ_j should satisfy

$$-\theta_{jm}\le\theta_j\le\theta_{jm} \tag{11}$$

Whenever the mechanism design satisfies equation (11), no singularity will exist.

4. Design of 2-dofs spherical manipulators with decoupled geometry

4.1 Type Design

The Type design of 2-dofs spherical manipulators is based on the general idea shown in figure 2. Using the 3R and 4R pairs in figure 3 to replace the F and P pairs separately, a new

structure (2R&8R manipulator) for figure 2(a) is constructed as shown in figure 9. Similarly, figure 10 shows the improved configuration of figure 2(b), a 2R&PRR manipulator, but distinguishingly, additional modification is that a through hole is added to the center of the revolute joint R_1, so the prismatic pair P can be set in the center of the hole and rotates with R_1. As a result, the workspace of θ_1 can reach 2π.

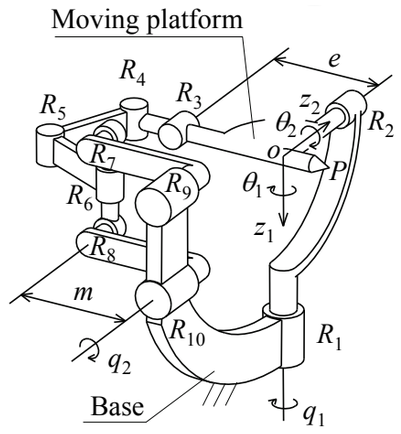

Fig. 9. 2R&8R manipulator

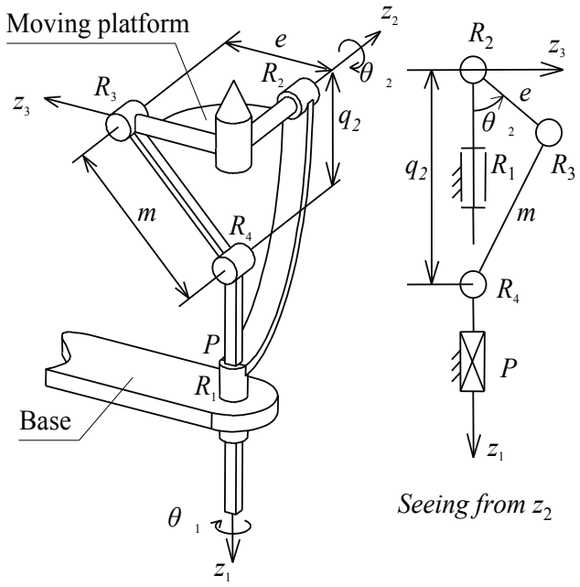

Fig. 10. 2R&PRR manipulator

4.2 Kinematics

Firstly, the 2R&8R manipulator in figure 9 will be discussed. Let e be the distance between the axes of R_2 and R_3, m be the distance between the axes of R_8 and R_{10} (or R_7 and R_9). Also, suppose that, when the moving platform is on the initial position, the axis of R_1 is perpendicular to the plane consisting of the axes of R_2 and R_3. Then the displacement relationships between input and output for the 2R&8R manipulator are:

$$\begin{cases} q_1 = \theta_1 \\ m\sin q_2 = e\sin\theta_2 \end{cases} \tag{12}$$

In the structure design, it is easy to set the length m of $\overline{R_7R_9}$ and $\overline{R_8R_{10}}$ equal to the distance e between the axes of R_2 and R_3 so as to get the one-to-one input-output mapping. Let $m = e$, it follows that:

$$\left.\begin{aligned} q_1 &= \theta_1 \\ q_2 &= \theta_2 \end{aligned}\right\} \tag{13}$$

This implies that the direct linear one-to-one input-output correlation, so the velocity jacobia matrix becomes an identity one.

Now we discuss the the 2R&PRR manipulator shown in figure 10. Suppose that the input parameters, q_1 and q_2, represent the angular displacement of the revolute joint R_1 and the distance between the axes of R_2 and R_4 separately. They are driven by a rotary actuator and a linear actuator. The pose of the moving platform is defined by the Euler angles θ_1 and θ_2 of the platform. Let e be the distance between the axes of R_2 and R_3, m be the distance between the axes of R_3 and R_4. Also suppose that, axis z_3 is through the point o and always perpendicular to the plane of z_1-z_2 and moreover, define the value of θ_2 is zero whenever the axis of R_3 is on the plane of z_1-z_2. Then the coordinates of R_4 and R_3 for the axes z_1 and z_3 are

$$\begin{cases} R_4(z_1, z_3) = R_4(q_2, 0) \\ R_3(z_1, z_3) = R_3(e\cos\theta_2, e\sin\theta_2) \end{cases} \tag{14}$$

The displacement relationship between input and output is:

$$\begin{cases} q_1 = \theta_1 \\ (q_2 - e\cos\theta_2)^2 + e^2\sin^2\theta_2 = m^2 \end{cases} \tag{15}$$

Taking the derivative of equation (15), it follows that

$$\begin{bmatrix} \dot{q}_1 \\ \dot{q}_2 \end{bmatrix} = J^{-1}\begin{bmatrix} \dot{\theta}_1 \\ \dot{\theta}_2 \end{bmatrix} \tag{16}$$

Where,

$$J = \begin{bmatrix} 1 & 0 \\ 0 & \dfrac{eq_2\sin\theta_2}{e\cdot\cos\theta_2 - q_2} \end{bmatrix} \tag{17}$$

4.3 Singularity and workspace

The 2R&8R manipulator shown in figure 9 has two legs. The first leg (R_1 to R_2) produces the Euler angle θ_1 of the platform by the input of q_1; while the second one (R_{10} to R_3) produces θ_2 by q_2. To illustrate the motional relationship, let us introduce a transition parameter z to equation (12), it follows that:

$$\begin{cases} q_1 = \theta_1 \\ m\sin q_2 = z = e\sin\theta_2 \end{cases} \tag{18}$$

where, z is the displacement of F-pair (R_4 to R_6) in the direction of z_1.
From equation (18), it is seen that the Euler angle θ_1 is produced from the input of q_1 directly by the first leg; while θ_2 is produced from q_2 by the second leg through two transformations, which include (1) rotary to linear motion $q_2 \Rightarrow z$ using $m \cdot \sin q_2 = z$, and (2) linear to rotary motion $z \Rightarrow \theta_2$ using $z = e \cdot \sin\theta_2$. In the second transformation, there exists a limitation related to friction circle. Let ρ denote the radius of the friction circle of R_2, which is determined by the product of the radius r of the revolute joint's axis and the equivalent friction coefficient μ as follows.

$$\rho = \mu r \tag{19}$$

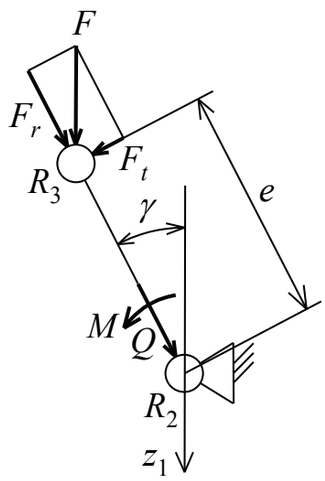

Fig. 11. Force and torque of R_2

Let γ denote the angle between z_1 and the link $\overline{R_2R_3}$, and decompose the force F into two parts, the radial component F_r and the tangent component F_t (see figure 11). Then the force F acts on R_2 is equivalent to a force Q and a torque M, which can be calculated from the following equations.

$$\left.\begin{aligned} Q &= F_r = F \cdot \cos\gamma \\ M &= F_t \cdot e = F \cdot e \cdot \sin\gamma \end{aligned}\right\} \tag{20}$$

As a basic law in mechanics, the effect of a force Q and a torque M acting on a rigid body is equivalent to a force Q_h with an offset h, which is shown in figure 12 and can be calculated as follows

$$\left.\begin{aligned} Q_h &= Q \\ h &= M / Q = e \cdot \tan\gamma \end{aligned}\right\} \tag{21}$$

where, h is the distance between the action lines of force Q_h and Q.

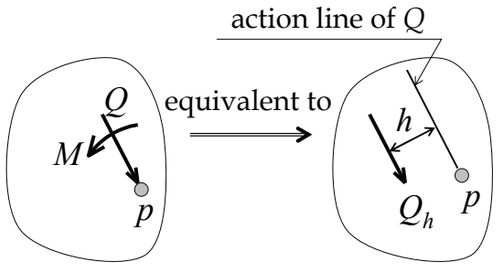

Fig. 12. Force couple equivalent

There exist three instances for the different relationship between h and ρ, which are (1) $h < \rho$, the revolute joint R_2 will never rotate regardless the value of Q_h; (2) $h > \rho$, revolute joint R_2 can rotate; and (3) $h = \rho$, the critical condition. In the critical condition of $h = \rho$, using equation (21), it follows that:

$$\gamma = \arctan(\rho / e) \tag{22}$$

Then the workspace of θ_2 satisfies:

$$-(\pi / 2 - \gamma) < \theta_2 < \pi / 2 - \gamma \tag{23}$$

On the other hand, the angle θ_1 produced by the first leg is limited only by the structure design of the F-pair and the base, so the workspace of θ_1 can reach a designated area through proper design. Assume that the workspace of θ_1 is from – $\pi/2$ to $\pi/2$, then the workspace of the spherical mechanism can be depicted by the reachable range of the point P as shown in figure 13. The workspace is smaller than a hemisphere, so it would be limitted in some applications.

When the mechanism is running, the direction of axis z_1 keeps unchanged, while the direction of axis z_2 alters according to θ_1. So the workspace represented by spherical surface in figure 13 can be interpreted as follows: point P draws latitude lines when only θ_1 changes and draws longitude lines while only θ_2 alters.

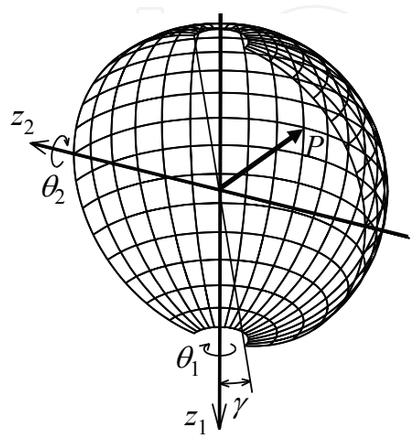

Fig. 13. The workspace denoted by the locus of point P

Now we examine the 2R&PRR manipulator in figure 10. The only limitation of this mechanism is caused by the friction circle of R_2. This limitation can be described by figure 14, from which we can see that the work space of θ_2 satisfies

$$\theta_{2\min} < \theta_2 < \theta_{2\max} \tag{24}$$

Where $\theta_{2\min}$ and $\theta_{2\max}$ are the minimum and the maximum boundaries, which can be simply calculated based on figure 14 as follows

$$\theta_{2\min} = \arcsin \frac{m\rho}{e\sqrt{\rho^2 + (\sqrt{e^2 - \rho^2} + m)^2}} > 0 \tag{25}$$

$$\theta_{2\max} = \arctan \frac{m - \sqrt{e^2 - \rho^2}}{\rho} + \arctan \frac{\sqrt{e^2 - \rho^2}}{\rho} < 2\pi \tag{26}$$

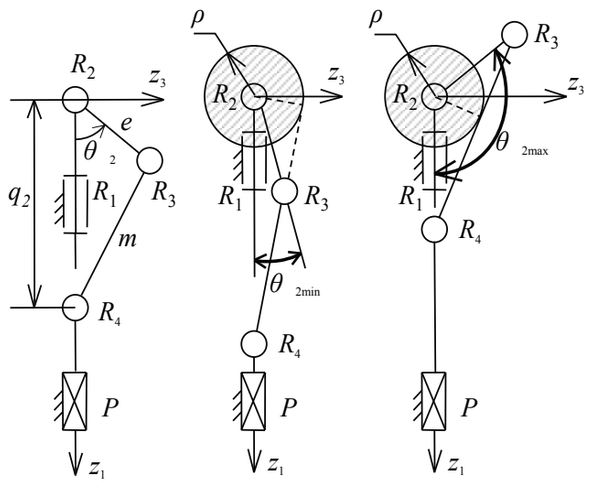

Fig. 14. Workspace of θ_2 limited by friction circle of R_2

It means that the workspace of the mechanism can not reach a hemisphere. Clearly, this is not desirable.

In fact, because the workspace of θ_1 is [0, 2π], the mechanism workspace can reach a hemisphere only if the workspace of θ_2 is chosen [0, $\pi/2$] or [$\pi/2$, π]. So there exist two methods to get a hemisphere workspace.

Figure 15 shows the critical instances for both of them; each one uses the similar technique to offset the axis of R_4 from the axis z_1. Let n denotes the axis offset of R_4 (or the length of AR_4), and n_c is the special value of n for the critical configurations as shown in figure 15, then n should be chosen equation (27). Using this technique, a hemisphere work space can be obtained.

$$n > n_c = \frac{m\rho}{e} \tag{27}$$

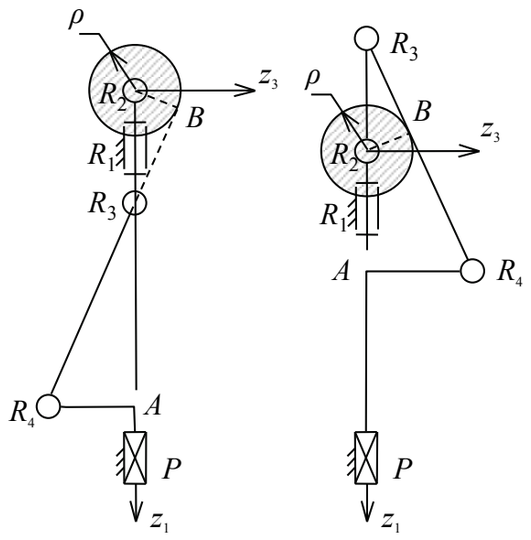

Fig. 15. Two methods to modify the boundaries of θ_2 : (a) $\theta_{2\min} = 0$, (b) $\theta_{2\max} = 2\pi$

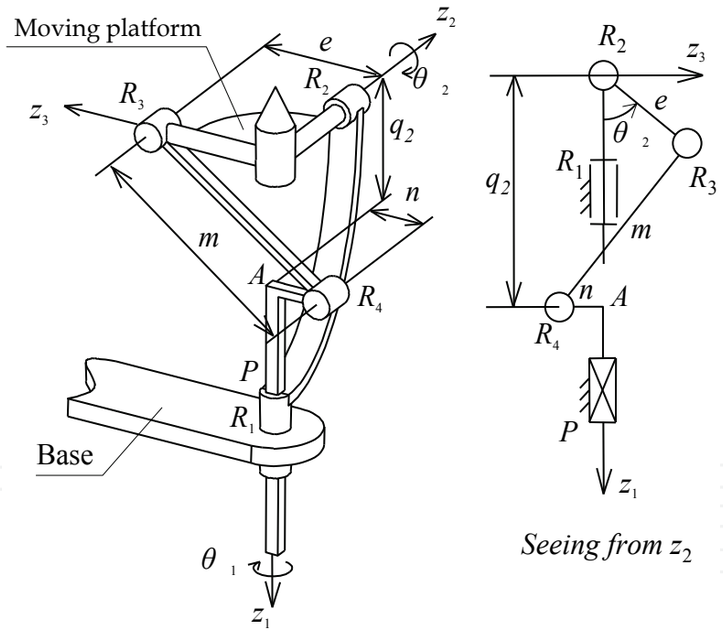

Fig. 16. The improved mechanism for $\theta_2 \in [0, \pi / 2]$

The improved architectures are shown in figure 16 and figure 17, in which the workspace of θ_2 includes the area of [0, π/2] or [π/2, π] separately.

A prototype model of the mechanism for the condition of $\theta_2 \in [0, \pi / 2]$ is designed. Figure 18 shows the outline picture of this model. In this design, one leg is actuated by a servo motor through a tooth belt; while the other leg is actuated by the other servo motor through

a ball screw, which converts the rotational movement into the translational one. Both motors are fixed on the base. Besides, another revolute joint R_5 is added to connect the prismatic pair with the nut of the ball screw.

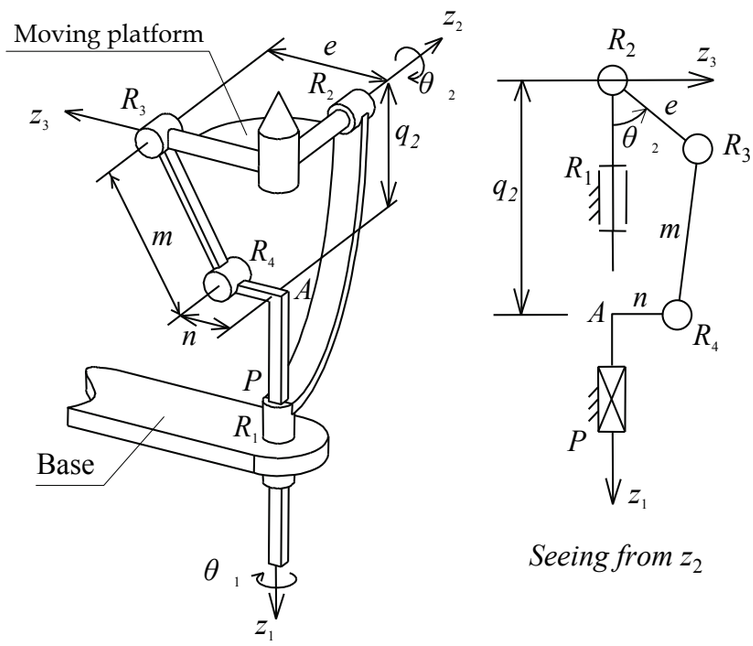

Fig. 17. The improved mechanism for $\theta_2 \in [\pi / 2, \pi]$

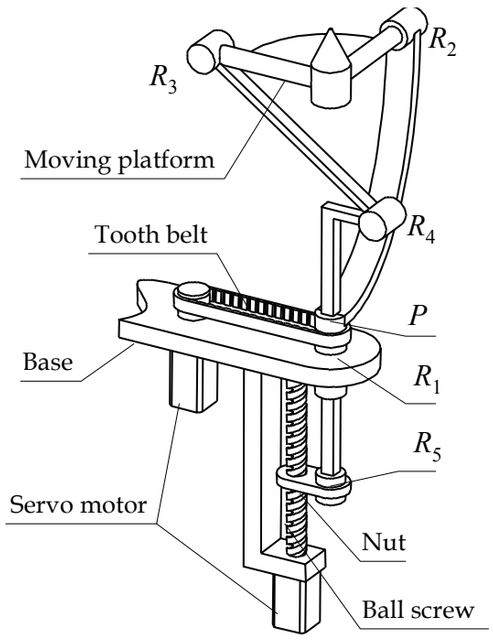

Fig. 18. The prototype model for $\theta_2 \in [0, \pi / 2]$

5. Conclusions

A general idea for type design of decoupled parallel manipulators with lower mobility is introduced. A unified frame for the type design is provided and divided into two independent aspects. Some kinds of decoupled parallel manipulators with 3-dofs pure translational and 2-dofs pure rotational movements are obtained.

6. Acknowledgement

The author gratefully acknowledges the financial support of the National Natural Science Foundation of China (No. 50475055).

7. References

Baron L. & Bernier, G. (2001). The design of parallel manipulators of star topology under isotropic constraint, 2001 ASME Design Engineering Technical Conferences, Paper No. DAC-21025, Pittsburgh, PA.

Carricato, M. & Parenti-Castelli, V. (2001a). A family of 3-DOF translational parallel manipulators, in: Proceedings of the 2001 ASME Design Engineering Technical Conferences, Pittsburgh, PA, DAC-21035.

Carricato, M. & Parenti-Castelli, V. (2001b). A two-decoupled-dof spherical parallel mechanism for replication of human joints, *Servicerob 2001 – European Workshop on Service and Humanoid Robots*, pp. 5–12, Santorini, Greece.

Carricato, M. & Parenti-Castelli, V. (2004). A Novel Fully Decoupled Two -Degrees-of-Freedom Parallel Wrist, *The International Journal of Robotics Research*, 23(6), 661-667.

Gao, F.; Zhang, Y. & Li, W.M. (2005). Type synthesis of 3-dof reducible translational mechanisms, *Robotica*, 23(2), 239-245.

Gogu, G. (2005). Fully-Isotropic Over-constrained parallel wrists with two degrees of freedom, *in Proceedings of 2005 IEEE International Conference on Robotics and Automation* (ICRA 2005), Barcelona, Spain , 18-22, ISBN 0-7803-8915-8 , pp. 4025-4030.

Hervé, J.M. & Sparacino, F. (1992). STAR: a new concept in robotics, *International Conference of 3K-ARK*, pp. 176–183.

Kim, H.S. & Tsai, L.W. (2003). Design optimization of a cartesian parallel manipulator, *Journal of Mechanical Design*, 125(1), 43–51.

Kong, X.W. & Gosselin, C. (2002). Kinematics and singularity analysis of a novel type of 3-CRR 3-dof translational parallel manipulator, *International Journal of Robotic Research*, 21(9), 791–798.

Li, W.M.; Gao, F. & Zhang, J.J. (2005a). R-CUBE, a Decoupled Parallel Manipulator Only with Revolute Joints, *Mechanism and Machine Theory*, 40(4), 467-473.

Li, W.M.; Gao, F. & Zhang, J.J. (2005b). A three-DOF translational manipulator with decoupled geometry, *Robotica*, 23(6): 805-808.

Li, W.M.; Zhang, J.J. & Gao, F. (2006a). P-CUBE, A decoupled parallel robot only with prismatic pairs, *The 2nd IEEE/ASME International Conference on Mechatronic and Embedded Systems and Applications*, Beijing, China.

Li, W.M.; Sun, J.G.; Zhang, J.J.; He, K. & Du, R. (2006b). A novel parallel 2-dof spherical mechanism with one-to-one input-output mapping, *WSEAS Transactions on Systems* 5(6).

Li, W.M.; He, K.; Qu, Y.X.; Zhang, J.J. & Du, R.(2007a). On the type design of a fully decoupled 2-DOF spherical mechanism with a hemisphere workspace, *WSEAS Transactions on Systems* 6(10).

Li, W.M.; He, K.; Qu, Y.X.; Zhang, J.J. & Du, R.(2007b). HEMISPHERE, a fully decoupled parallel2-DOFspherical mechanism. *Proceedings of the 7th WSEAS int. Conference on Robotics, Control and Manufacturing Technology*, 301-306, Hangzhou, China.

Tsai, L.W.; Walsh, G.C. & Stamper, R. (1996). Kinematics of a novel three DOF translational platform, *Proceedings of the 1996 IEEE International Conference on Robotics and Automation*, pp. 3446–3451, Minneapolis, MM.

Tsai, L.W. (1996). kinematics of a three-DOF platform manipulator with three extensible limbs, *Recent Advances in Robot Kinematics*, J. Lenarcic, and V. Parenti-Castelli, ed., pp.401–410, Kluwer Academic Publishers, London.

Zhang, J.J.; Li, W.M.; Wang, X.H. & Gao, F. (2006a). Study on kinematics decoupling for parallel manipulator with perpendicular structures. *Proceedings of the 2006 IEEE/RSJ International Conference on Intelligent Robots and Systems*, 748-753, Beijing, China.

Zhang, J.J.; Wang, X.H.; Li, W.M. & Gao, F. (2006b). On the study of type design for PMWPSs and their kinematics characteristics. *WSEAS Transactions on Systems* 5(6): 1328-1334.

Zhang, J.J.; Wang, X.H.; Li, W.M. & Gao, F. (2006c). Mechanism Design for 3-, 4-, 5- and 6-DOF PMWPSs. *Proceedings of the 6th WSEAS International Conference on Robotics, Control and Manufacturing Technology*, 93-98, Hangzhou, China.

Zhao, T.S. & Huang Z. (2000). A novel three-DOF translational platform mechanism and its kinematics, *2000 ASME Design Engineering Technical Conferences*, Paper No. MECH-14101, Baltimore, MD.

Parallel Manipulators, New Developments

Edited by Jee-Hwan Ryu

ISBN 978-3-902613-20-2

Hard cover, 498 pages

Publisher I-Tech Education and Publishing

Published online 01, April, 2008

Published in print edition April, 2008

Parallel manipulators are characterized as having closed-loop kinematic chains. Compared to serial manipulators, which have open-ended structure, parallel manipulators have many advantages in terms of accuracy, rigidity and ability to manipulate heavy loads. Therefore, they have been getting many attentions in astronomy to flight simulators and especially in machine-tool industries.The aim of this book is to provide an overview of the state-of-art, to present new ideas, original results and practical experiences in parallel manipulators. This book mainly introduces advanced kinematic and dynamic analysis methods and cutting edge control technologies for parallel manipulators. Even though this book only contains several samples of research activities on parallel manipulators, I believe this book can give an idea to the reader about what has been done in the field recently, and what kind of open problems are in this area.

InTech Europe

University Campus STeP Ri
Slavka Krautzeka 83/A
51000 Rijeka, Croatia
Phone: +385 (51) 770 447
Fax: +385 (51) 686 166
www.intechopen.com

InTech China

Unit 405, Office Block, Hotel Equatorial Shanghai
No.65, Yan An Road (West), Shanghai, 200040, China
中国上海市延安西路65号上海国际贵都大饭店办公楼405单元
Phone: +86-21-62489820
Fax: +86-21-62489821

IntechOpen